Grating angular displacement transducer using a Fabry-Perot structure

Li zhiquan*[a] , Qiang xifu[a] , Wu zhaoxia*[b] , Fan lina[b]
[a]Harbin institute of technology, Harbin 150001 CHN
[b]Yanshan University,Qinghuangdao 066004,CHN

ABSTRACT

A novel grating angular displacement transducer using a multiplex Fabry-Perot interference technology has been developed. The Fabry-Perot interferometer (FPI) has been traditionally used to examine either small spectral ranges or relatively simple spectra. Recently, however,the studies have shown that the FPI can be competitive with the Michelson interferometer over extended spectral ranges. A relatively new FPI is described based on two gratings.

Keywords: Angular-movement transducer , Fabry-Perot Interferometer, Grating, Transducers

1. INTRODUCTION

The interferometer based on the Fabry-Perot interference technology has been used historically at high resolution either to examine an elementary spectrum, containing only a few lines or to examine a small spectral region that has been isolated by a filter of other dispersive device[1]~[6].When larger spectral regions or complex high-resolution spectra are required, the instrument of choice has been the Michelson interferometer or the Fourier transform spectrometer(FTS).However, recent studies[1]-[4]have challenged this choice. These authors pointed out correctly that the inversion of a Fabry-Perot interferometer(FPI)is competitive with a Michelson interferometer over an extended spectral range. Yet in one of these studies there has been some limitation that is related to the application technique and the theory. In this paper, we have first reviewed the method of grating measuring angular displacement, and then introduced the grating angular displacement transducer using a Fabry-Perot structure.

2. PRINCIPLE AND STRUCTURE

2.1 Transducer Using Grating

National Engineering Laboratory (NEL.1966) developed a measuring system that uses an optical grating with shaft encoders[5]. The accuracy of the complete system is determined by the highly accurate optical grating.
The system is unique in the method used to relate the encoder and grating signals. The system was used interpolation of the grating pitch described above to increase the resolution or the shaft encoder and provide some sensing logic.
Fig.1(a)shows a relationship between the grating division and the encoder resolution which indicates that a

In *Optical Sensing, Imaging, and Manipulation for Biological and Biomedical Applications*, Robert R. Alfano, Ping-Pei Ho, Arthur E. T. Chiou, Editors, Proceedings of SPIE Vol. 4082 (2000) • 0277-786X/00/$15.00

precise mechanical relationship is required between the encoder and the grating if ambiguity is to be avoided at the transition points of the encoder.

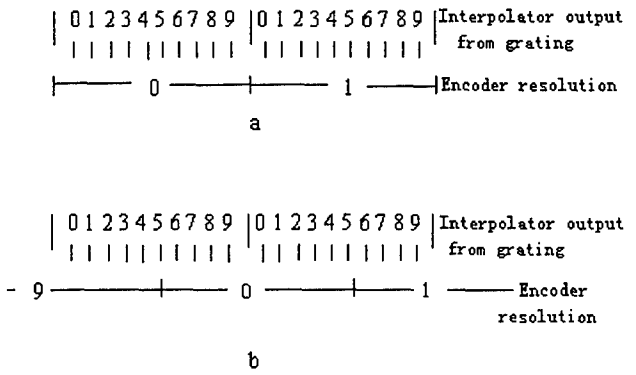

Fig.1 grating and encoder relationship

This requirement is avoided in the NEL system by modifying the relationship to that shown in Fig.1(b). The encoder track and the grating division needed now only have an accuracy up to $\pm 1/2$ for a division of the grating, providing this tolerance is not exceeded over the whole length of the grating. The encoder is interrogated only during the transition of the interpolator output from 0 to 9 or from 9 to 0, i.e. at each grating division. Other, coarser tracks of the encoder can be interrogated in a similar manner.

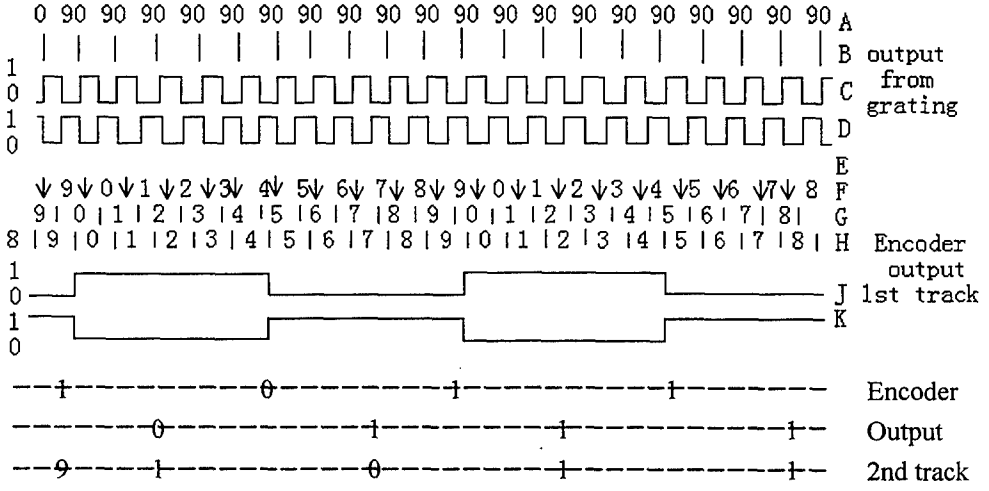

Fig.2 Interrogation of grating-encoder combination

The system described by Russell is detailed in Fig.2. The upper four rows are the output and the derived outputs form the grating. Row A represents the cycle of output form the grating divisions, e.g. each cycle representing 0.1 mm for a 10 lines/mm grating. Row B represents the ten subdivisions generated by the interpolator, each

subdivision representing 0.01 mm. Row C is a "lead" line which is a square wave at the same rate, grating output and is a logic "1" for counts of 0 to 4 of the interpolator output, and logic"0" for counts 5 to 9. Row D is a "lag" line and is the inverse of row C.Rows E to K represent the signals derived from the shaft encoder which is of conventional from having binary or gray code output which can, if required, be decoded into decades. Fig.3 shows the first stages of such a unit with a grating of 10 lines/mm of displacement with a resolution of 0.10mm. It would be providing a resolution of 1 part in 100 000 and only require mechanical assembly and tolerances which are easily obtained.

The method shown is for a decade readout, but, for purely digital readout, the interpolator output can be decoded to provide the required digital code and the shaft encoder output can be left in a digital code. The lag/lead signals are generated with respect to the main grating divisions which are the same as the least significant bits on the shaft encoder.

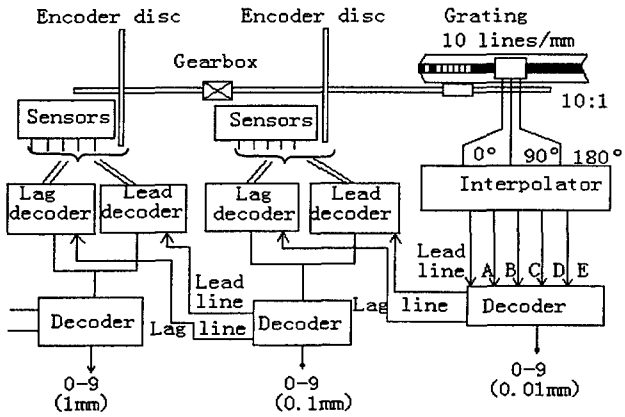

Fig.3 Grating-encoder system

2.2 Fabry-Perot Structure and Theory

First, let us begin our discussion of FPI by illustrating the optical configuration and by describing the operation of the instrument.The basic FPI is shown in Fig.4.Radiation entering into the instrument passes first through a prefilter to isolate a modest spectral region to be examined by the grating.There are two grating is the Fig.4. One is movable grting,the other is fixed grating.The fixed grating acts as a comb filter with a comb separa-tion in the spectrum that is dependent on the separation of the plates. As the movable grating moves small angular displacement, the spectral resolution increases. At the end of the scan, when the movable grating have been moved a small angular displacement that depends on the desired resolution, the high-frequency portion of the spectrum is identified. We note that during the motion of the grating the parallelism must be maintained to a small fraction of the wavelength of the radiation examined. During the motion of the movable grating, the signal from a simple interferometer can be characterized by the integral expression[6].

$$N_i = \frac{A_0 \Omega}{4\pi} Q_e T_{oi} \int T_f(\lambda) T_{et}(\lambda, t) \mathrm{B}_{\mathrm{atmos}}(\lambda) d\lambda \qquad (1)$$

Where the fixed grating transmission[2] can be expressed as the series

$$T_{et}(\lambda,t)=[(1-R)/(1+R)]\{1+2\sum_{n=1}^{\infty}R^{n}D_{n}\mathrm{COS}[4\pi n\,\mu t\,\lambda\mathrm{COS}(Q)]\} \tag{2}$$

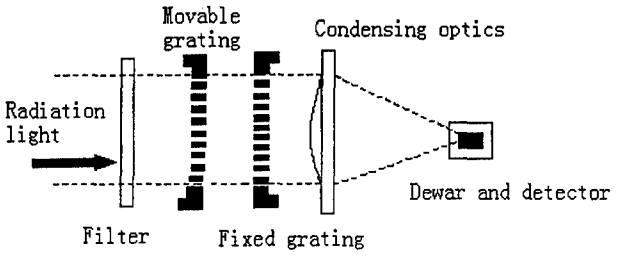

Fig4 Optical elements of the FPI

In Eqs.(1)and (2), A_0 is the area of the seam of the gratings; Ω_i is the solid angle subtended by the detector; Q_e is the quantum efficiency of the detector; T_{oi} is the system transmission coefficient for all elements except the fixed grating and filter; T_f is the system transmission of the filter; R is fixed grating reflecting; n is an index related to the number of reflections within the two grating cavities; D_n is the defect function (which is 1.0 for a perfect instrument); t is the distance between the grating; μ is the index of refraction; θ is angle of movable grating moving; λ is wavelength; $B_{atmos}(\lambda)$is the brightness per unit wave number of the radiation.

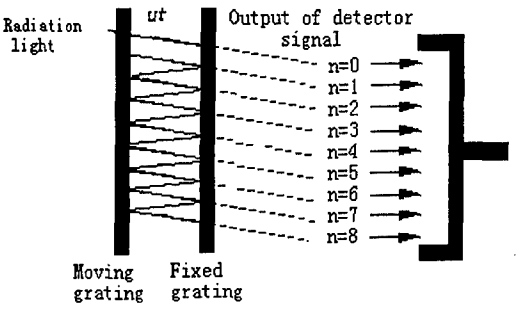

Fig. 5 The signal of FPI modulation

Such as Fig.5, the analysis can be simplified if the fixed grating is oriented at normal to the path of the incident radiation.i.e.,

$$N_I = f(\theta) \tag{3}$$

Then,

$$\theta = N_i^{-1} \tag{4}$$

where N_i^{-1} is the inverse function.

3.RESULTS

The results obtained by passing a computer-generated spectrum through the above FPI transform equations show that this analytical technique can be useful for the high accuracy angular displacement measuring. In our simulations, we found that it is relatively easy to limit the instrumental broadening and to resolve small spectral features, while the required grating motion remains quite short compared with that of a FTS(Fourier Transform spectrometer).For test purposes, we chose to examine a simulated spectrum from the region near 21.88 cm^{-1}. This region of the spectrum contains a nearly random distribution of several strong ozone lines.

Fig.6 is a comparison of the individual harmonic terms from a 20 cm scan[1]. One can see that the higher-harmonic

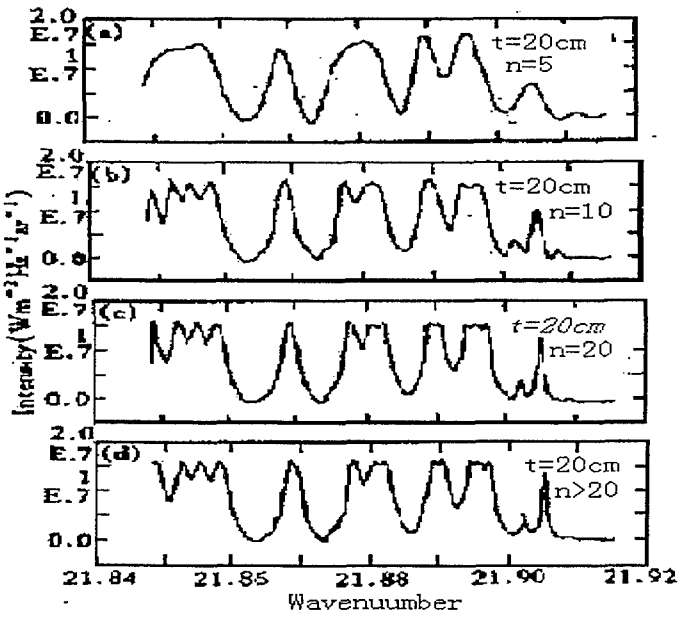

Fig.6 The output of the transducer

terms, e.g., n = 20, are much less broader than that of the lower harmonics,such as n = 5. The higher-harmonic terms of the FPI are equivalent to a longer scan distance for a Michelson interferometer: the 20th harmonic of a 20cm FPI scan has an equivalent Michelson path length of 4 m. One should note that the data in these figures have been normalized to permit comparison; in practice the signal from the higher harmonics is weaker than that from the lower harmonics as the result of reflective losses. Consequently, the higher harmonics must be weighted with the lower harmonics in such a way as to produce a spectrun with little broadening but with enough signal that the minor features can be resolved.

4.CONCLUSION

In this paper we have illustrated a new analysis technique for the FPI. It was shown previously that a FPI can be used as a Michelson interferometer by changing the separation between the gratings by examining the first harmonic, using Fourier Transform spectroscopy. It has also been shown that ,with FPI,the necessary scan distance is a factor of 10 less that needed by a Michelson interferometer to achieve the same spectral resolution. Angular displacement is normal problem. But , after we confine it with FPI,a novel instrument has been developed.

REFERENCES

1. Paul B. Hays and Hilaiy E. Snell, Multiples Fabry-perot interferometer, APPLIED OPTICS, Vol. 30, No. 22, August 1991, (3108-3113).
2. Claude belleville and Gaetan Duplain White-light interferometric multimode fiber-optic strain sensor, OPTICS LETTERS/Vol. 18, No. 1/January 1, 1993 (78-80).
3. Stephen T. West and Chib-Lin Chen, APPLIED OPTICS/Vol. 28, No. 19/1 October 1989, (4206-4209).
4. Chia-Chen Chang and Jim Sirkis Multiplexed Optical Fiber Sensors Using a Single Fabry-Perot Resonator for Phase Modulation, JOURNAL OF LIGHTWAVE TECHNOLOG. VOL. 14, NO. 7, JULY 1996, (1653-1663).
5. Anatoli A. Chtcherbakov and Pavel V. Bulkin Long dual-cavity fiber optic Fabry-Perot strain

sensor with rugate mirrors, Optical Engineering, Vol, 35 No. 4, April 1996(1059-1063).
6. T. W. Kao and H. F. TaylerHigh-sensitivity intrinsic fiber-optic Fabry-Perot pressure sensor, April 15, 1996/Vol. 21, No. 8/OPTICS LETTERS.
7. S. F. Masri, M. S. Agbabian, A. M. Abdel-Ghaffar, M. Higazy, R. O. Claus, and M. J. deVries, Experimental study of embedded fiber-optic strain gauges in concrete structures , Jaurnal of Engineering mechanics, 1994. Vol. 20, No. 8(1696-1717).
8. Murphy, K., Fogg, B. R., and Vengsarkar, A. M., Spatially weighted vibration sensors using tapered two-mode optical fibers, J. Lightwave Technol, Vol. 10, No. 11(1680-1687).
9. Y. J. Rao, P. J. Henderson, N. E. Fisher and D. A. Jackson, Wavelength division multiplexed in-fibre Bragg grating Fabry-Perot sensor system for quasi-distributed current measurement, Appl. Opt. Div. Conf. , Brighton, 16-19 March 1998.
10. Kersey A D, Berkoff T A and More W W , Multiplexed fibre Bragg gratingstrain-sensor system with a fibre Fabry-Perot wavelength filter, Opt. lett. 18(1370-1372) 1993.